Journal of Agriculture and Environment
Vol. 20 No. 1, 2024: 321-336

Assessment of land surface temperature and factors influencing urban green space dynamics in Sapele, Delta State of Nigeria

D.A. Akintunde-Alo, A. Joy and O.O. Komolafe

Department of Social and Environmental Forestry, University of Ibadan, Nigeria

ABSTRACT

Forest is a carbon sink contributing to the tropical Land Surface Temperature (LST) changes. However, information on the nexus between Urban Green Space (UGS) and LST of most cities is limited. Therefore, spatiotemporal variability in UGS and LST, and factors affecting UGS dynamics were examined in Sapele, Delta State, Nigeria. Landsat imageries of 2002, 2012, and 2022 were obtained and classified using Iso Cluster Classification with point pixel-based correction for accuracy improvement. The LST was extracted from the imageries. Relationship between NDVI and LST was established using R. Structured questionnaire was used to elucidate information on factors affecting UGS (FAUGS); population growth (PG), lack of law enforcement (LLE), demand for timber (DT), agricultural expansion (AE), overgrazing (O), soil characteristics (SC), urban sprawl (US) and lack of land tenure system (LLTS), using logit regression at $\alpha=_{0.05}$. Four LULC were identified; UGS, water bodies, bare land, and built-up areas. The UGS decreased from 88.55% in 2002 to 81.83% in 2022, built-up area expanded from 4.64% to 12.55%. Highest mean LST (27.46°C) and lowest NDVI (0.54) were recorded in 2012, least LST (26.46°C) and highest NDVI (0.69) were recorded in 2002. Negative nexus was observed between NDVI and LST for 2002 (-0.453), to 2022 (-0.393). The odd ratio showed that PG ($1.2x10^8$), US (13.8), and LLTS (3.0) significantly affected UGS dynamics with the regression model (FAUGS) = -9.7 + 18.6(PG) – 8.0(LLE) - 23.61(DT) - 18.5(AE) -10.8(O) - 25.7(SC) + 2.6(US) + 1.1(LLTS). This study affirmed that urban green space was affected by urbanization.

Keywords: Urban vegetation; satellite image; Iso cluster classification

INTRODUCTION

Publicly management of the vegetative areas within an urban environment such as forested areas, wilderness, street trees, backyard gardens, coaster areas, and gardens simply means urban greenspace (McIntyre *et al*., 2008). Urban green space (UGS) plays a significant role in the economic, sociological, and physiological well-being and livelihood of urban society (Nwatu *et al*., 2021; Okikiola and Alo, 2020). However, UGS is greatly affected due to physical development in cities, which is capable of harming the microclimate condition of the city and further resulting in severe conditions in the environmental biotic cycle ((Nwatu

Correspondence: danielakintundealo@gmail.com
https://dx.doi.org/10.4314/jagrenv.v20i1.30

et al., 2021; Li *et al*., 2016). Understanding the relationship between UGS and land surface temperature (LST) will help to know the variation in urban temperature and also provide the earth science range of themes and issues on human-environmental interaction and global environmental changes (Faqe and Ibrahim, 2017). LST is the radiative skin temperature of the land surface derived from solar radiation in vegetated areas (Qin *et al.*, 1999). Most contemporary cities generally lack green space owing to irrational transformation due to anthropogenic activities such as deforestation, construction works, urban developments, and population growth (Okikiola and Alo, 2020). This irrational transformation has resulted in radical variations in the biophysical state of the earth's surface, leading to the loss of habitats, forest land destruction, and subsequently disturbances of natural heat transfer between the land and atmosphere (Grimmond, 2007). A promising way to solve this environmental problem is by examining LULC as related to geographical change (Akter *et al.*, 2021). Remote sensing (RS) and Geographical Information Systems (GIS) approaches have been useful tools in the monitoring of such environmental phenomena which are more efficient than ground-based data collection (Borges *et al.*, 2006). The purpose of RS and GIS in detecting LULC in the field of research cannot be overemphasized as it is an indispensable tool in almost every environmental endeavour.

Understanding LULC and LST and their effects on the health of the ecosystem is essential to making significant advances in documenting the rate and cause of changes in LULC and the effect of these changes on LST (Atubi *et al*., 2018). Linkages between LULC derived from satellite imagery and LST have been revealed by many studies, that the increase in LST is a result of the changes in land use patterns owing to unplanned urban expansion, population growth or rapid urbanization (Alademomi *et al*., 2020; Bokaie *et al*., 2016). Orimoloye *et al*. (2018) noted that the prolonged effect of an increase in LST could have serious health implications on human life due to alterations in the layer of the atmosphere. Empirical information on the relationship between Urban heat Inland (UHI) and the identified factors of land use land cover changes will help in giving detailed spatiotemporal measures capable to showing insight on associations degree between the factor and the phenomena Agbaogun and Akintunde-Alo (2020).

LULCC in many regions poses a great challenge to the sustainability of the environment which thus necessitated the need for assessing the biophysical parameters and determining the changes over time (Akter *et al.*, 2021). Sapele LGA which is one of the ancient `towns in Delta State has witnessed an increase in population growth and urbanization which has gradually resulted in vegetation area reduction (Iortyom *et al.*, 2022). Agbaogun and Akintunde-Alo (2020), also reiterated that inadequate effective measures in the land use land cover pattern are a major contributor to global warming, climate change, and urban heat islands. Inadequate current and updated information about urban green changes are major driving factors toward poor environmental planning and management. In recent times studies have proven that there is a relationship between vegetal loss and surface temperature in the tropics (Nwatu *et al.*, 2021; Okugini, 2020). In Sapele LGA studies emphasizing the perceived factors that could be responsible for this observed relationship is generally limited. Due to the dearth of studies regarding relationship between LULC and LST with the factors responsible for the changes in the urban green space in this study area, this study was set to achieve this by evaluating the extent and trend between urban green space and land surface temperature and also giving detailed information on the perceived factors responsible for the changes with the view to updating information on the status and trend pattern of LULC which can be reckoned upon for management of urban green space in the study area.

MATERIALS AND METHODS

Study Area

Sapele LGA is one of the 25 local government areas in Delta State and the administrative headquarters is located in the central senatorial zone of Sapele. Sapele LGA is geographically located between latitudes 5° 42' and 5° 57' N and between longitudes 5° 33' and 5° 45'E (Figure 1). Sapele is a coaster town located on the southern fringe of the Ethiope River that flows through the area and the river is wide, deep, and safe enough that can be sailed on by ships or boats. Sapele LGA covers a total land area of 450.55 km^2. The mean temperature of Sapele LGA ranges between 25˚ C to 35 ˚ C with an annual rainfall pattern ranging between 2500 mm to 3000 mm elongating from March to November (Ajokporise, 2011). Sapele LGA is walled by heavy vegetation and thick forest. The major occupations are predominantly farmers and artisans.

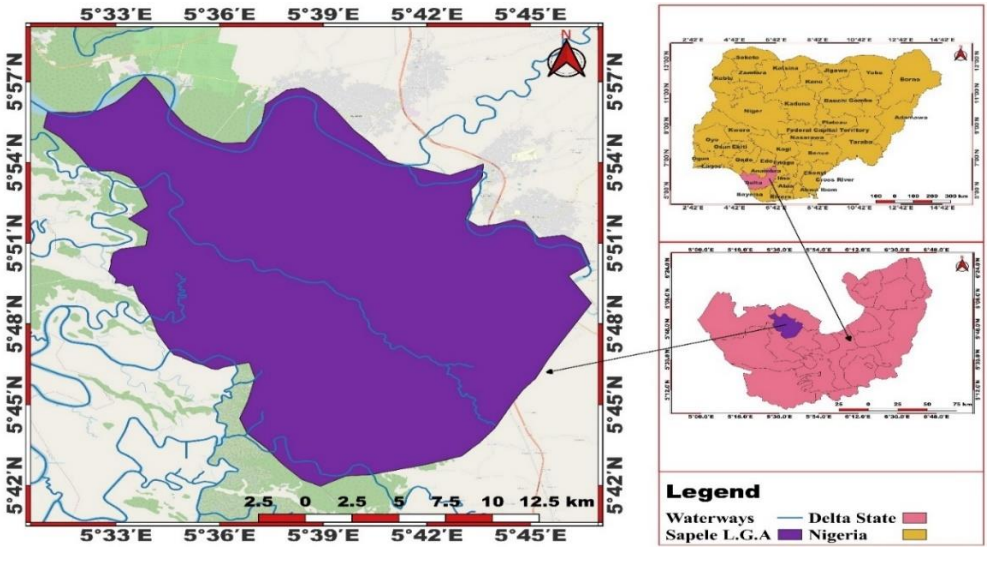

Figure 1: Sapele Local Government Area of Delta State, Nigeria

Data Collection

Data collected for this study involved both primary and secondary data. The primary data involved the use of Questionnaires which were administered using Google Docs with a series of questions which was directed to people who resided in the study area towards obtaining information on the perceived factors that are responsible for the urban green space changes in Sapele LGA. The secondary data used for this study involves downloading Landsat satellite imageries of 2002, 2012, and 2022 from the United States Geological Survey website' (www.earthexplorer.usgs.gov). The year selected for this study was based on the availability of Landsat images that were available with low cloud. Details of the Landsat data downloaded are presented in Table 1.

Table 1: Details of the satellite imagery acquired

Satellites	Year/ Month/ Date	Sensor Identify	Path/Row	Spatial Resolution
Landsat 7	2002/12/8	ETM+	188/55	30m
Landsat 7	2012/12/25	ETM+	188/55	30m
Landsat 8	2022/12/29	OLI/TIR	188/55	30m

Where: (ETM+ and OLI/TIR) are 'Enhanced Thematic Mapper plus; 'Operational Land Imager/Thermal Infrared Radiation'.

Data Analysis

The data acquired were analysed using ARCGIS 10.8, Quantum GIS (QGIS) 3.28 and R statistical package, and the classification was done following Anderson's (1976) image classification scheme of land cover techniques. In selecting the band for image analysis band combinations of 2, 3, and 4 (green, red, and near-infrared) were used for Landsat 7 while for Landsat 8, band combinations of 3, 4, and 5 (green, red, and near-infrared) were used by applying false colour composite (FCC) to select the region of interest for the land cover category. The Iso Cluster Classification (ICC) procedure as used by Hu *et al*. (2023); and Ismail *et al*. (2020) was used in classifying the LULC pattern for the study area. The ICC was used for this study due to its ability to discover patterns and features that may not be obvious or predefined when picking training samples for supervised classification.

Post-Reclassification Techniques for ICC

The first step involves the use of reclassifying tools of the spatial analyst to reclassify the image into the desired number of classes, while the Image pixel-based or class-based controls correction techniques was used to improve the accuracy of ICC of the final map out. All the LULC carried out using the ICC algorithm was converted from raster to points. The grid point was overlayed on high-resolution imageries (Google satellite) as used by Hu *et al*. (2023) to reclassify the wrongly classified pixels into the correct land cover classes using a raster field calculator.

Change Detention Analysis

A change detention examination was carried out and the rate of changes over the years assessed for the study area was determined. The percentage change for each year and the rate of change between the years were all calculated using the formula below.

The change was computed following Alo *et al*. (2020)

Change $(\Delta) = Y_2 - Y_1$ ..... Equation 1

The average rate of change (AVR) was computed using the formula below

$\text{AVR} = \frac{Y_2 - Y_1}{T_2 - T_1}$ ..... Equation 2

Percent Change Per Year (%Δ/yr.) was computed using this formula below

$\%\Delta/\text{yr.} = \frac{Y_2 - Y_1}{Y_1}$ ..... Equation 3

Where Δ represents change; Y_2 and Y_1 are the area sizes in the initial year T_1 and final year respectively.

Normalize Difference Vegetation Index (NDVI)

The degree of greenness for the study area was determined using NDVI with values ranging between +1 and -1. The NDVI was computed following Rouse *et al*. (1974).

$NDVI = \frac{NIR-Red}{NIR+Red}$…… Equation 4

Accuracy Assessment

Accuracy assessment is a means of evaluating the quality of the image analysis carried out for either supervised or unsupervised algorithms (Hu *et al*., 2023; Kaur and Singh, 2015). As such, 30 ground control points (GCP) for Water bodies, bare land, vegetation, and built-ups giving rise to a total of 120 sample points created to validate if the pixels are right sampled into the correct land cover classes for the years 2002, 2012, and 2022. The GCP was loaded on high-resolution imagery (Google Earth Pro), and historical imagery options on Google Earth Pro in the view option were used for the years 2002 and 2012. Error matrices were generated from the pixel of the classified imagery with the ground truth data from Google Earth. The User accuracy, producer accuracy, and overall accuracy were calculated from the error matrices for each land use using the following equations:

User Accuracy = $\frac{Total\ Number\ of\ Correctly\ Classified\ Pixels\ in\ each\ Category}{Total\ Number\ of\ Classified\ Pixels\ in\ that\ Category} \times 100$.. Equation 5

Producer Accuracy = $\frac{Total\ Number\ of\ Correctly\ Classified\ Pixels}{Total\ Number\ of\ reference\ Pixels\ in\ that\ Category} \times 100$.....Equation 6

Overall Accuracy = $\frac{Total\ Number\ of\ Correctly\ Classified\ Pixels\ (Diagonal)}{Total\ Number\ of\ Reference\ Pixels} \times 100$ …..Equation 7

Kappa Coefficient = $\frac{(TS*TCS)-\sum(\sum Column\ Total \times Row\ Total)}{TS^2-\sum(Column\ Total \times Row\ Total)} \times 10$……..…..…Equation 8

Land Surface Temperature Determination

The land surface temperature for the study area was estimated using the steps below:

Conversion of Digital numbers into spectral radiance:

The satellite sensors measure the reflectance from the earth's surface as digital numbers (DN) representing every pixel of the image. The DN data from Landsat was converted using the spectral radiance scaling factors provided in the metadata file:

Conversion of Digital Number (DN) to Top of Atmosphere Radiance (TOA) using

$L\lambda = M_L \times Q_{cal} + A_L$ ……Equation 9

$L\lambda$ is the spectral radiance at the sensor [W/(m^{2}srμm)]
M_L represents the band-specific multiplicative rescaling factor
Q_{cal} is the level of 1-pixel value in DN for Band 10
A_L is the band-specific additive rescaling factor (0.1)

Conversion of spectral radiance into at-sensor brightness temperature:

By applying the inverse of the Planck function, thermal bands' radiance values will be converted to a brightness temperature value using the equation below.

This is the satellite temperature in Kelvin.

$B_t = [\frac{K_2}{\left(\ln\left(\frac{K_1}{L\lambda}+1\right)\right)}]$ - 273.15……. Equation 10

Where: B_t = Top of Atmosphere brightness temperature (° Kelvin), Lλ =Top of Atmosphere radiance [W/(m²srμm)], K1=Band-specific thermal conversion constant from the metadata (K1_CONSTANT_BAND_x, where x is the thermal band number), K2 = Band-specific thermal conversion constant from the metadata (K2_CONSTANT_BAND_x, where x is the thermal band number).

Calculation of NDVI for Emissivity Correction

NDVI is a simple graphical indicator usually used to analyse remote sensing measurements and assess if the observed target includes green vegetation or not. NDVI is one of the outputs that run into the model to retrieve LST

$NDVI = \frac{B_{NIR}-B_R}{B_{NIR}+B_R}$ ……. Equation 11

Where: B_{NIR} represents a near-infrared band of the satellite imagery, B_R represents the red band of the satellite imagery

The proportion of Vegetation (P_v)

$Pv = \left(\frac{NDVI-NDVI_{min}}{NDVI_{max}-NDVI_{min}}\right)^2$ ……. Equation 12

Emissivity

$E = 0.004 * P_v + 0.986$ ……. Equation 13

Retrieving the Land Surface Temperature/Emissivity-Corrected Land Surface Temperature (TS)

$TS = \frac{Bt}{1+\left[\left(\frac{0.00115\ x\ Bt}{1.4388}\right) x\ Ln(E)\right]}$……. Equation 14

Where: TS = Land Surface Temperature, Bt = Top of Atmosphere brightness temperature, E = Emissivity

Relationship between Land Surface Temperature (LST) and NDVI

Correlation and regression analysis between LST and Normalized Difference Vegetation indices (NDVI) in the study was computed using linear regression and Pearson Product Moment of Correlation (PPMP) 'r' analysis on R. Correlation and regression analysis are statistical methods used to measure the level of relationship or association between two variables and the strength of the relationship. The coefficient of the correlation varies between +1 and -1. A value of +1 correlation coefficient indicates a perfect positive degree of relationship between the two variables, and a value of -1 correlation coefficient indicates a perfect negative degree of relationship between the two variables, while correlation coefficient values of zero indicate that there is no linear relationship between the two variables (Add references).

Determination of Perceived Factor of UGS

The responses obtained from the questionnaire were subjected to binary logit regression. The equation used was (FAUGS)= PI + PG +LLE +DT + AE + O +SC + LLT + SC + US. Where FAUGS = Factor affecting urban green space; PI = Population increase; LLE = lack of law enforcement; DT= Demand for timber; AE = Agricultural expansion; O = Overgrazing; SC = Shifting cultivation; LLT = Lack of land tenure system; SC = Soil characteristics; US = Urban sprawl. Various factors that contributed significantly to the Urban Green spaces were determined.

RESULTS

Sapele Local Government Area covers a total land area of approximately 450.55 km^2. The land use land pattern has significantly changed. The changes observed between the years 2002 to 2022 are evidence of alteration due to the change patterns from one land use to the other (Figures 2, 3, and 4). Vegetation was more evident in 2002, which gradually reduced in 2012 but the reduction in the vegetation covered in 2022 was more pronounced when compared with 2012. Table 2 shows the area and the percentages for all the LULCs in all the years assessed. The area occupied by vegetation in 2002 was 398.96 km^2 (88.55%), built-up areas accounted for 20.92km^2 (4.64%) while water bodies and bare land in 2002 covered an area of 12.03 km^2 (2.67%) and 18.64km^2 (4.14%) respectively. However, there was an increase in the area occupied by built-up, bare land and water bodies from 2002 to 2012 as it changed from 20.92km^2 (4.64%) to 22.35km^2 (4.96%), 12.03 km^2 (2.67%) to 22.13 km^2 (4.91%) and 12.03 km^2 (2.67%) to 12.06km^2 (2.68%) respectively, but a decrease in the area occupied by vegetation was observed from 2002 to 2012 with a value of 398.96 km^2 (88.55%) to 394.02 km^2 (87.45%). Between 2002 to 2022 the vegetation and bare land significantly reduced by 6.73% (398.96 km^2 to 368.66 km^2) and 1.3% (18.64 km^2 to 12.64 km^2) respectively. Built-up and water bodies recorded 7.91% and 0.15% increases between 2002 to 2022 of (20.92 km^2 to 56.55 km^2) and (12.03 km^2 to 12.70 km^2) respectively.

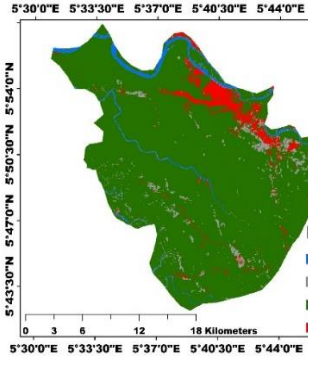

Figure 2: The LULC in 2002

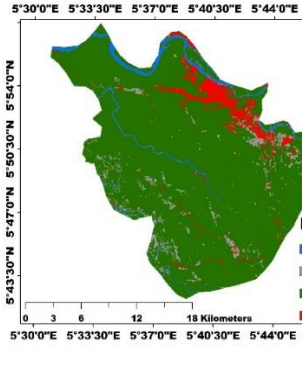

Figure 3: The LULC in 2012

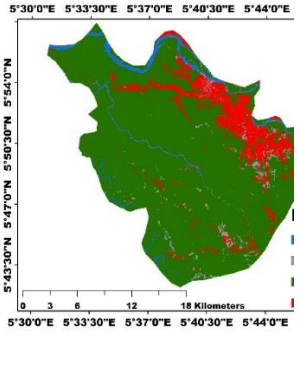

Figure 4: The LULC in 2022

Table 2: Land cover classification for the study area (2002 - 2022)

LULC 2002	Area 2002	Area %	Area 2012	Area %	Area 2022	Area %
Water bodies	12.03	2.67	12.06	2.68	12.70	2.82
Bare land	18.64	4.14	22.13	4.91	12.64	2.81
Vegetation	398.96	88.55	394.02	87.45	368.66	81.83
Built up	20.92	4.64	22.35	4.96	56.55	12.55
TOTAL	450.55	100	450.55	100	450.55	100

Land Use Land Cover Change Trend

A negative change (-4.95km^2) was observed in the vegetation cover between 2002 and 2012, which decreased further (-25.35km^2) between 2012 to 2022, making a net decrease of 30.30km^2 in 20 years (Table 3). However, the built-up areas increased between 2002 to 2012 with 1.43km^2, while a surge increase of 34.20 km^2 was observed between 2012 to 2022 accounting for total of 35.63 km^2 increment in the built-up area within the period of 20 years. Between year 2002 to 2012 an increase of 0.03km^2 was observed in the water bodies, from 2012 to 2022 the water bodies increased by 0.64 km^2 making a total increase in the area occupied by water bodies with 0.67 km^2 within the study period. A positive change was observed in bare land between 2002 to 2012 (3.49 km^2), from 2012 to 2022 and a decrease of -9.49 km^2 was observed indicating a net loss of -6 km^2 within the period of 20-year study.

However, the average rate of change between 2002 to 2012 indicated a negative value for vegetation and bare land of -8.22 km^2/yr. and -0.09 km^2/yr. respectively while water bodies and built-up areas were found to be positive with a value of 0.01 km^2/yr. and 8.30 km^2/yr. respectively. The average rate of change (AVR) observed from the year 2002 down to 2022 shows a reduction in the areas occupied by vegetation while bare land increased between 2002 to 2012 but decreased between 2012 -2022 and 2002 to 2022 with values of -0.60 and -0.95 respectively. However, AVR observed from the year 2002 down to 2022 shows an increment in the areas occupied with built-ups as the average rate of change, between 2002 to 2012, 2012 to 2022, and 2002 to 2022 was 0.14, 3.56, and 3.42 respectively. An increase was observed between AVR of change between 2002 to 2012 in bare land (0.35) but decreased between 2012 to 2022 (-0.95) and 2002 to 2022(-0.65).

Table 3: LULC classification between 2002 and 2012

LULC	Change 2002 - 2012	Change 2002 - 2022	Change 2012 - 2022	A.R.C 2002 - 2012	A.R.C 2002 - 2022	A.R.C 2012 - 2022	% C/Yr. 2002 - 2012	% C/Yr. 2002 – 2022	% C/Yr. 2012 – 2022
Water bodies	0.03	0.67	0.64	0.00	0.07	0.06	0.22	5.55	5.32
Bare land	3.49	-6.00	-9.49	0.35	-0.60	-0.95	18.73	-32.17	-42.87
Vegetation	-4.95	-30.30	-25.35	-0.49	-3.03	-2.54	-1.24	-7.59	-6.43
Built up	1.43	35.63	34.20	0.14	3.56	3.42	6.84	170.33	153.03

Normalized Difference Vegetation Index (NDVI)

The NDVI (Normalized Difference Vegetation Index) was utilized to examine the relationship amid spectral variability and vegetation growth rate changes. The spatial distribution of the NDVI for all the years examined in this study are presented in Figure 5 to 7. The highest NDVI value (0.69) was observed in the year 2002 followed by year 2022

(0.57) while year 2012 had NDVI value of 0. 54. However, the lowest NDVI value was found in 2012 with a value of -0.26 followed by year 2022 and 2002 with a value of -0.15 and -0.08 respectively.

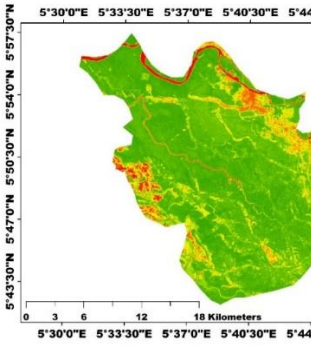

Figure 5: The NDVI for 2002

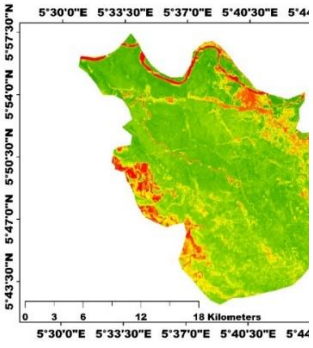

Figure 6: The NDVI for 2012

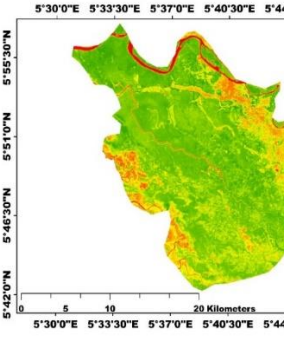

Figure 7: The NDVI for 2022

Accuracy Assessment of LULC classification

The summary of the error matrix of the accuracy assessment showed that overall accuracy for each of the years 2002, 2012, and 2022 were 97.5%, 96%, and 94.5%, respectively (Table 4). The kappa statistic for the years 2002, 2012, and 2022 was 96.7 %, 94.7% and 93%, respectively.

Table 4: Accuracy assessment of 2002, 2012 and 2022 error matrix

LULC	2002			2012			2022		
	UA	PA	OA	UA	PA	OA	UA	PA	OA
Water bodies	100	100		100	100		100	100	
Built-Ups	95	96		95	92		93	93	
Vegetation	98	98	97.5	94	97	96	91	96	94.5
Bare land	97	97		95	95		95	90	
Kappa statistic	96.7			94.7			93		

UA: User Accuracy, PA: Producer Accuracy, OA: Overall Accuracy

Spatio-temporal Pattern of Land Surface Temperature (LST) for the Study Area

The spatial distribution of land surface temperature for 2002 revealed that the value ranges between 22.84°C to 48.93°C (Figure 8), while the mean temperature for the year 2002 was observed to be 26.46°C. However, the spatial distribution of land surface temperature for 2012 ranges between 22.85°C to 48.96°C, and the mean temperature recorded for the year 2012 was 27.46°C (Figure 9). The spatial distribution of land surface temperature for 2022 revealed that the value ranges between 22.22°C to 50.16°C (Figure 10) and the mean temperature observed for the year 2022 was 26.54°C. Distribution of highest, lowest and mean land surface temperature (LST) and Normalized difference vegetation indices (NDVI) for all land use types were identified (Table 5). Distribution of highest, lowest and mean LST

and NDVI for all land use types in Sapele L.G.A show that built-ups in 2002, 2012 and 2022 recorded the highest distribution of LST which gradually increased from 48.93 °C to 48.96 °C and 50.16 °C respectively. The mean LST for all the land use types also indicated that built-up and bare land areas had the highest mean temperature value while water bodies and vegetation had the lowest mean temperature value respectively. However, the mean NDVI for the land use types in the years 2002, 2012, and 2022 was higher in vegetated areas than other land uses. But the lowest mean NDVI value was observed on the water bodies, followed by built-up and bare land respectively.

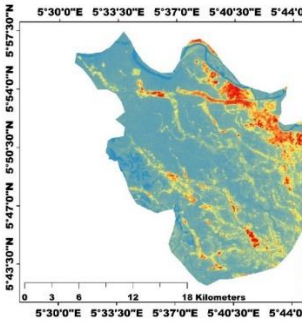

Figure 8: The LST for 2002

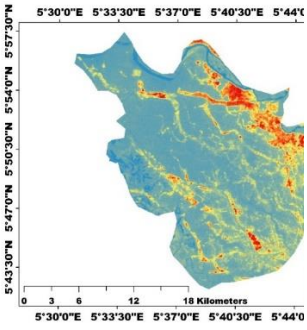

Figure 9: The LST for 2012

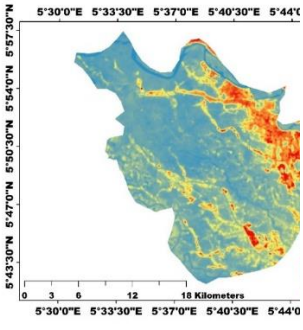

Figure 10: The LST for 2022

Table 5: Distribution of LST, NDVI highest, lowest and mean for all land use type in Sapele L.G.A for years 2002, 2012, and 2022

LULC		2002		2012		2022	
		LST	NDVI	LST	NDVI	LST	NDVI
Vegetation	High	35.23	0.69	34.99	0.54	45.01	0.50
	Low	22.84	-0.07	22.85	-0.23	22.22	-0.01
	Mean	25.36	0.54	26.09	0.27	26.02	0.27
Built-Ups	High	48.93	0.48	48.96	0.39	50.16	0.29
	Low	25.08	0.19	25.09	-0.26	23.18	-0.08
	Mean	31.95	0.27	31.87	0.06	30.31	0.17
Water bodies	High	36.77	0.48	36.78	0.40	32.86	0.12
	Low	23.12	-0.09	23.13	-0.25	23.69	-0.067
	Mean	24.57	0.12	24.57	-0.06	24.78	0.02
Bare land	High	39.03	0.46	39.05	0.46	35.78	0.23
	Low	23.69	0.08	23.69	-0.20	23.91	-0.02
	Mean	30.75	0.31	29.82	0.12	30.01	0.13

Correlation Analysis for LST and Land NDVI

Correlation analyses carried out for the study years are shown in Table 6. The correlation coefficients for the years 2002, 2012, and 2022 were negative correlations of -0.453, -0.263, and -0.393 respectively. All the tested LST and NDVI for each year show a negative relationship which is statistically significant at alpha level of < 0.000. The scatter

plot of LST against NDVI for each year is presented in Figures 11 to 13. The R^2 values for 2002, 2012, and 2022 range from 0.2302, 0.1316 and 0.146 respectively.

Table 6: Correlation matrix between LST and NDVI

	LST 2002	NDVI 2002	LST 2012	NDVI 2012	NDVI 2022	LST 2022
LST 2002	1					
NDVI 2002	-0.453 (<.001)	1				
LST 2012	0.001 (.685)	0.002 (.178)	1			
NDVI 2012	-0.001 (.687)	-0.000 (.867)	-0.263 (<.001)	1		
NDVI 2022	-0.002 (.188)	0.003 (.032)	-0.000 (.779)	0.001 (.405)	1	
LST 2022	-0.000 (.853)	-0.002 (.186)	-0.000 (.748)	-0.002 (.235)	-0.393 (<.001)	1

Computed correlation used the Pearson method with listwise-deletion.

Perceived Factors that influence UGS in the study area

Table 7 shows the logit regression model carried out on the perceived factors that influenced changes in the UGS in the study area. The model generated was (FAUGS)= -9.7 + 18.6(PG) – 8.0(LLE) - 23.61(DT) - 18.5(AE) -10.8(O) - 25.7(SC) + 2.6(US) + 1.1(LLTS), indicated that PG ($1.2x10^8$), US (13.8) and LLTS (3.03) significantly affected UGS dynamics.

Table 7: Logistic binary regression model of perceived factors that influence UGS

	Estimate	Odds ratio (unit ch)	Odds ratio (range)
Const.B0	-9.71	0.00	
PG	18.64	124245800.00	124245800.00
LLE	-7.98	0.00	0.00
DT	-23.61	0.00	0.00
AE	-18.54	0.00	0.00
O	-10.81	0.00	0.00
SC	-25.66	0.00	0.00
LLT	1.10	3.01	3.03
SC	-1.89	0.15	0.15
US	2.62	13.77	13.77

Where FAUGS = Factor affecting urban green space; PI = Population increase; PG = Population growth; LLE = lack of law enforcement; DT= Demand for timber; AE = Agricultural expansion; O = Overgrazing; SC = Shifting cultivation; LLT = Lack of land tenure system; SC = Soil characteristics; US = Urban sprawl.

DISCUSSION

LULC pattern for this study area was performed using ICC classification, this was done due to its ability to discover patterns and features that may not be obvious or predefined

(Hu *et al*., 2023). The accuracy of ICC can be improved to have a higher accuracy level in the LULC analysis using the Image pixel-based or class-based control correction approaches. However, the limitation of this method is the time taken in selecting the points that were wrongly classified for a particular land use type and also the need for the researcher to know the area to be classified when grouping pixels with common characteristics produced from the algorithm to be related with the ground picture (Hu *et al*., 2023). However, ICC and Image pixel-based were used to perform the LULC analysis for this study. The analysis shows a gradual reduction of vegetation cover in the urban green space of Sapele L.G.A, this could be attributed to alteration in different land use types. The evidence of the alteration was seen in the urban green space reduction between 2002 to 2022, which could be a result of population growth or rural-to-urban drift. This was also reported by Akter *et al.* (2021) that population growth, economic factors as well and migration of people were the major driving factors of urban green space dynamics. Furthermore, the gradual spread of built-up areas from 2002 to 2022 has resulted in massive vegetation loss. Okugini (2020) reported a similar trend and noted that Delta State built-up areas kept increasing in various years used in his research, which was also attributed to development. Furthermore, the continuous decrease in the vegetative cover observed in sapele between 20 years in this study area was also elucidated from a questionnaire that was administered to the people who resided in the study area. Sapale LGA has witnessed changes over the years owing to Urban sprawl, industrialization, Population growth, and lack of land tenure. This factor contributed significantly to urban green space losses. This is an indication that an increase in the factor level of significance will have an impact on the land use land cover for the study area. This is in line with Hansen *et al*. (2013) findings on spatial and non-spatial forest area changes where they reiterated that LULC changes are a result of population growth, poverty, overcrowding, agricultural land expansion, lack of law enforcement and lack of land tenure system are the major contributors to forest cover decline in their study areas. This was also corroborated by Okikiola and Alo (2020), that the changes in Urban green space in the Ado metropolis were significantly affected by factors ranging from poverty, lack of law enforcement, increase in population, demand for timber, and migration from rural to urban drift.

The spatial distribution of land surface temperature in Sapele LGA from 2002 to 2022 indicated that the highest temperature was in year 2022, followed by 2012, while the lowest temperature was observed in 2002. The increase in the observed surface temperature for this study area could be attributed to an increase in human activities in the urban green space. This finding agrees with Nwatu *et al*. (2021), that the increase in human population and its co-activities on UGS is alarming and a threat to the natural environment. On the other hand, a reduction in UGS over the years tends to give rise to a slight increase in temperature due to a reduction in carbon sequestered by the UGS during photosynthesis. Nastaran (2014) concluded that tree planting is an effective way to mitigate the heat island effect and the consequences of increased temperatures resulting from climate change on human earth. Forest cover loss or replacements of green spaces with impermeable materials owing to urbanization and industrialization will make it difficult to trap some of the heat, thereby radiating the heat back into the space and leading to an increase in temperature (Nwatu *et al*., 2021; Shahzad and Riphah, 2015). Furthermore, Pal and Ziaul, (2017); Fashae *et al*. (2020); and Tyubee (2021) also reported that the transformation or replacement of evapotranspiration land cover materials with impervious materials decrease the atmospheric humidity with the prolonged effect capable of leading to global warming increase.

The temperature variability per land use cover classes for this study indicated that built up have the highest temperature as well as the highest mean temperature value closely followed by bare land across the entire year studied in this research. The high mean values observed for these two classes are a result of the replacement of the vegetal areas with impermeable materials, paved surfaces, and open surfaces. Wardana (2015) also reiterated that the average temperature of any given area is predisposed by the decrease or increase in built-up area and vegetation cover comparatively and cumulatively. This is an implication that an increase in built-up areas is bound to hurt the temperature. The lowest temperature per land-use class was observed on the water bodies due to its evaporative cooling effect, followed by the vegetation, which could be attributed to the phenomena known as the cooling effect of vegetation. The low temperature observed on the UGS could be a result of its various environmental functions ranging from shade, evapotranspiration, albedo, air circulation, and carbon dioxide absorption. Many researchers have opined that Lower LST are frequently found in areas with high NDVI but areas with less NDVI are often associated with high LST value. Variability in temperature of different land cover types is a result of the presence of metal, built-ups, and structures which are capable of affecting the amount of radiation received and emitted by urban infrastructure. This finding was in agreement with Okikiola and Alo (2020) findings in Spatio-Temporal Dynamics of Urban Green Space and Temperature in Ado-Ekiti Metropolis as their findings indicated that built-up and bare soil had the highest temperature while water bodies and vegetation were observed to be the lowest mean temperature. This finding was also corroborated by Orimoloye *et al.* (2018) that the built-up and bare land areas recorded the highest LST value in all the years examined in their study area as well.

The relationship between the UGS and LST from 2002 to 2022 in this study area shows a moderate negative correlation which are both significant at an alpha level of 0.001. This finding agrees with Weng *et al* (2014) in modelling annual parameters of clear-sky land surface temperature variations and evaluating the impact of cloud cover using time series of Landsat TIR data in Los Angeles County, California Los Angeles where they observed that the relationship between LST and NDVI shows a strong negative correlation and significant at alpha 0.001. However, the difference between the moderate correlation observed in this study and the strong correlation observed in their study could be a result of variations in the climatic conditions, the terrain, and the topology between the study area. The level of significance observed in this research simply means that the LST and the UGS values are statistically different from each other, an indication that the decrease in UGS will significantly increase the land surface temperature of Sapele LGA. In other words, the increase in LST could be tied to the reduction in the vegetated area (Okikiola and Alo, 2020). The negative correlation observed in this study is in line with Nwatu *et al*. (2021) that there is a negative correlation between LST and NDVI in their study area. However, it should be noted that the UGS changes can weaken the urban heat effect. This was also corroborated by Awuh *et al*. (2019) that the incessant transformation of land cover greatly influences the spatial distribution of land surface temperature which is capable of resulting in urban heat Island when the temperature of an urban region is higher than its rural surroundings.

The accuracy mapping of LULC using the iso-clustered algorithm method of classification for the image analysis was found to be of higher accuracy in the study area which is also reflected in the NDVI and LST output. This was in concord with Akter *et al*., (2021) who noted that the combined method of unsupervised, LST, and NDVI accuracy depict a high level of accuracy in their study area. The perceived factor that influences

changes in the UGS in the study area is population increment, population growth, lack of land tenure system, and urban sprawl. This study therefore affirmed that urbanization and population growth will further result in more vegetation loss, if necessary, measures such as urban green space management, urban plantation, home garden, and green walls concept practice are not put in place.

CONCLUSION

This study focused on the relationship between land use land cover changes and land surface temperature in Sapele L.G.A of Delta state. The decrease in the urban green space in the study area was a result of population growth, which led to consequence increase in the built-up area within the metropolis between 2002 and 2022. Furthermore, the land surface temperature of the study area also witnessed an increase, which could be articulated to an increase in the built-up and bare land due to changes in land use. Findings from this study showed that urban and population growth significantly influenced the reduction in dynamics of urban green space in Sapele L.G.A which is more vulnerable to changes as the impact of changes is more pronounced on the vegetation in the analysis carried out.

Based on the research carried out, the following recommendations are hereby made: the creation of awareness on the importance of greening and formulation of stringent urban green space policies that will forestall incessant removal of vegetation without replacement. The results documented in this study can be useful in studying and estimating weather phenomena such as microclimate, heat pockets, and maximum temperature in Sapele LGA

REFERENCES

Agbaogun, S.O. and Akintunde-Alo, D. (2020). *Research Square*, pp 1-12 https://orcid.org/0000-0002-6698-0385

Ajokporise, D. (2011). Perception and impact of climatic variations on crop production in Sapele local government area of Delta state, Nigeria. *Journal of Research in National Development*, *9*(1), 131-137.

Akter, T., Gazi, M.Y. and Mia, M.B. (2021). Assessment of land cover dynamics, land surface temperature, and heat island growth in northwestern Bangladesh using satellite imagery. *Environmental Processes*, *8*, 661-690.

Alademomi, A.S., Okolie, C.J., Daramola, O.E., Agboola, R.O. and Salami, T.J. (2020). Assessing the relationship of LST, NDVI and EVI with land cover changes in the Lagos Lagoon environment. *Quaestiones Geographicae*, *39*(3), 111-123.

Alo, A.A., Adetola, A.A. and Agbor, C.F. (2020). Modelling forest cover dynamics in Shasha Forest Reserve, Osun State, Nigeria. *Journal of Agriculture and Environment*, *16*(1), 129-142.

Atubi, A.O., Awaritefe, D.O. and Toyon, A.B. (2018). Analysis of land use and land cover change characteristics in Warri metropolis, Nigeria. *International Journal of Development and Sustainability*, *7*(3), 1143-1168.

Awuh, M.E., Japhets, P.O., Officha, M.C., Okolie, A.O. and Enete, I.C. (2019). A correlation analysis of the relationship between land use and land cover/land surface temperature in Abuja Municipal, FCT, Nigeria. *Journal of Geographic Information System*, *11*(01), 44.

Bokaie, M., Zarkesh, M.K., Arasteh, P.D. and Hosseini, A. (2016). Assessment of urban heat island based on the relationship between land surface temperature and land use/land cover in Tehran. *Sustainable Cities and Society*, *23*, 94-104.

Borges, C.K., de Medeiros, R.M., Ribeiro, R.E., dos Santos, É.G., Carneiro, R.G. and dos Santos, C.A. (2016). Study of biophysical parameters using remote sensing techniques to Quixeré-CE region. *Journal of Hyperspectral Remote Sensing*, *6*(6), 283-294.

Faqe Ibrahim, G.R. (2017). Urban land use land cover changes and their effect on land surface temperature: Case study using Dohuk City in the Kurdistan Region of Iraq. *Climate*, *5*(1), 13.

Fashae, O.A., Adagbasa, E.G., Olusola, A.O. and Obateru, R.O. (2020). Land use/land cover change and land surface temperature of Ibadan and environs, Nigeria. *Environmental monitoring and assessment*, *192*, 1-18.

Grimmond, S.U.E. (2007). Urbanization and global environmental change: local effects of urban warming. *The Geographical Journal*, *173*(1), 83-88.

Hansen, M.C., Potapov, P.V., Moore, R., Hancher, M., Turubanova, S.A., Tyukavina, A., Thau, D., Stehman, S.V., Goetz, S.J., Loveland, T.R. and Kommareddy, A. (2013). High-resolution global maps of 21st-century forest cover change. *Science*, *342*(6160), 850-853.

Hu, Y., Raza, A., Syed, N.R., Acharki, S., Ray, R.L., Hussain, S., Dehghanisanij, H., Zubair, M. and Elbeltagi, A. (2023). Land use/land cover change detection and NDVI estimation in Pakistan's Southern Punjab Province. *Sustainability*, *15*(4), p.3572.

Iortyom, E.T., Semaka, J.T. and Kargbo, P. (2022). The effect of urban expansion on peripheral agricultural lands in Makurdi City. *European Journal of Development Studies*, *2*(4), 100-108.

Ismail, M.A., Ludin, A.N.M. and Hosni, N. (2020). Comparative assessment of the unsupervised land use classification by using proprietary GIS and open-source software. *In*: *IOP Conference Series: Earth and Environmental Science* (Vol. 540, No. 1, p. 012020). IOP Publishing.

Jaeger, J.A., Bertiller, R., Schwick, C., Cavens, D. and Kienast, F. (2010). Urban permeation of landscapes and sprawl per capita: New measures of urban sprawl. *Ecological Indicators*, *10*(2), 427-441.

James, M. M., and Mundia, C. N. (2014). Dynamism of land use changes and surface temperature in Kenya: A case study of Nairobi City. *International Journal of Science and Research*, 3(4), 020131389.

Kaur, A., Sharma, N. and Singh, S. (2015). Assessment of different classification algorithms over LULC rugged terrain satellite imagery. In *IEEE Second International Conference on Signal Processing and Communication (ICSC-2015)* (Vol. 1, pp. 345-350).

Komolafe, O.O., and Akintunde-Alo, D.A. (2022). Geospatial modelling of Akure forest reserve in Ondo State, Nigeria. *Forest and Forest Product Society*. 346-357

Li, X., Mitra, C., Dong, L. and Yang, Q. (2018). Understanding land use change impacts on microclimate using weather research and forecasting (WRF) model. *Physics and Chemistry of the Earth, Parts A/B/C*, *103*, 115-126.

Li, Y., Zhao, M., Mildrexler, D.J., Motesharrei, S., Mu, Q., Kalnay, E., Zhao, F., Li, S. and Wang, K. (2016). Potential and actual impacts of deforestation and afforestation on land surface temperature. *Journal of Geophysical Research: Atmospheres*, *121*(24), 14-372.

McIntyre, N.E., Knowles-Yánez, K. and Hope, D. (2008). Urban ecology as an interdisciplinary field: differences in the use of "urban" between the social and natural sciences. *Urban Ecology: An International Perspective on the Interaction between Humans and Nature*, 49-65.

Nastaran Shishegar (2014). The impact of green areas on mitigating urban heat island effect. *International Journal of Environmental Sustainability*, 9(1), 119-130.

Njoku, E.A. and Tenenbaum, D.E. (2022). Quantitative assessment of the relationship between land use/land cover (LULC), topographic elevation and land surface temperature (LST) in Ilorin, Nigeria. *Remote Sensing Applications: Society and Environment*, *27*, 100780.

Nwatu, U.J., Alo, A.A. and Agbor, C.F. (2021). Temperature variability and impact of vegetation cover in Ibadan Metropolis, Ibadan, Nigeria. *Journal of Agriculture and Environment*, *17*(1), 161-175.

Okikiola, M.A. and Alo, A.A. (2020). Spatio-Temporal Dynamics of Urban Green Space and Temperature in Ado-Ekiti Metropolis, Nigeria. *Forests and Forest Products Journal*, *20*, 40-53.

Okugini, N.I. (2020). Analysis of land use/land cover change using geospatial techniques in Ukwuani Local Government Area of Delta State, Nigeria. *International Journal of Research and Innovation in Social Science (IJRISS)*, 4(3), 281 – 290

Orimoloye, I.R., Mazinyo, S.P., Nel, W. and Kalumba, A.M. (2018). Spatiotemporal monitoring of land surface temperature and estimated radiation using remote sensing: Human health implications for East London, South Africa. *Environmental Earth Sciences*, *77*, 1-10.

Pal, S. and Ziaul, S.K. (2017). Detection of land use and land cover change and land surface temperature in English Bazar urban centre. *The Egyptian Journal of Remote Sensing and Space Science*, *20*(1), pp.125-145.

Qin, Z. and Karnieli, A. (1999). Progress in the remote sensing of land surface temperature and ground emissivity using NOAA-AVHRR data. *International journal of remote sensing*, *20*(12), 2367-2393.

Rouse Jr, J.W., Haas, R.H., Deering, D.W., Schell, J.A. and Harlan, J.C. (1974). *Monitoring the vernal advancement and retrogradation (green wave effect) of natural vegetation* (No. E75-10354)

Shahzad, U., Riphah. (2015). Global warming: Causes, effects and solutions. *Durreesamin Journal*, *1*(4).

Tyubee, B. T. (2021). Estimating Per Capita Land Use/Land Cover Change (LULCC) in Makurdi, Northcentral Nigeria. *Urban Studies and Public Administration* 4(1), 97 – 109. http://dx.doi.org/10.22158/uspa.v4n1p97

Wardana, I.K. (2015). *Analysis of urban surface temperature for green spaces planning in Bandung city, Indonesia* (Master's thesis, University of Twente).

Weng, Q. and Fu, P. (2014). Modelling annual parameters of clear-sky land surface temperature variations and evaluating the impact of cloud cover using time series of Landsat TIR data. *Remote Sensing of Environment*, *140*, pp.267-278.